The Plant Cell, Vol. 17, 2314–2326, August 2005, www.plantcell.org © 2005 American Society of Plant Biologists

IRREGULAR TRICHOME BRANCH1 in Arabidopsis Encodes a Plant Homolog of the Actin-Related Protein2/3 Complex Activator Scar/WAVE That Regulates Actin and Microtubule Organization

Xiaoguo Zhang,[a] Julia Dyachok,[b] Sujatha Krishnakumar,[a,1] Laurie G. Smith,[b] and David G. Oppenheimer[a,2]

[a] Department of Botany and University of Florida Genetics Institute, University of Florida, Gainesville, Florida 32611-8526
[b] Section of Cell and Developmental Biology, University of California, San Diego, La Jolla, California 92093-0116

The dynamic actin cytoskeleton is important for a myriad of cellular functions, including intracellular transport, cell division, and cell shape. An important regulator of actin polymerization is the actin-related protein2/3 (Arp2/3) complex, which nucleates the polymerization of new actin filaments. In animals, Scar/WAVE family members activate Arp2/3 complex-dependent actin nucleation through interactions with Abi1, Nap1, PIR121, and HSCP300. Mutations in the *Arabidopsis thaliana* genes encoding homologs of Arp2/3 complex subunits PIR121 and NAP1 all show distorted trichomes as well as additional epidermal cell expansion defects, suggesting that a Scar/WAVE homolog functions in association with PIR121 and NAP1 to activate the Arp2/3 complex in Arabidopsis. In a screen for trichome branching defects, we isolated a mutant that showed irregularities in trichome branch positioning and expansion. We named this gene *IRREGULAR TRICHOME BRANCH1* (*ITB1*). Positional cloning of the *ITB1* gene showed that it encodes SCAR2, an Arabidopsis protein related to Scar/WAVE. Here, we show that *itb1* mutants display cell expansion defects similar to those reported for the *distorted* class of trichome mutants, including disruption of actin and microtubule organization. In addition, we show that the scar homology domain (SHD) of ITB1/SCAR2 is necessary and sufficient for in vitro binding to Arabidopsis BRK1, the plant homolog of HSPC300. Overexpression of the SHD in transgenic plants causes a dominant negative phenotype. Our results extend the evidence that the Scar/WAVE pathway of Arp2/3 complex regulation exists in plants and plays an important role in regulating cell expansion.

INTRODUCTION

The control of plant cell shape is of central importance to plant development. Because plant cells are surrounded by a cell wall, the problem of cell shape control can be reduced to the study of how directional cell expansion is controlled. *Arabidopsis thaliana* trichomes are an established model for how directional cell expansion leads to a specific three-dimensional shape (Schwab et al., 2000; Szymanski et al., 2000; Wasteneys, 2000; Smith, 2003). A cell biological approach to understanding trichome shape control has determined that the microtubule cytoskeleton is most important at the earliest stages of trichome development, including trichome branching (Mathur et al., 1999). Microtubule involvement in trichome branching is well supported by the finding that some of the genes identified by mutations that affect branch number encode proteins associated with the microtubule cytoskeleton. These proteins include a kinesin-like protein (Oppenheimer et al., 1997), a katanin-like protein (Burk et al., 2001), and α-tubulin (Abe et al., 2004). The involvement of the actin cytoskeleton in controlling directional cell expansion in trichomes has received much recent attention. Earlier pharmacological studies of trichome expansion established that the actin cytoskeleton plays a crucial role in controlling the direction of the rapid expansion that takes place after branches are initiated (Mathur et al., 1999; Szymanski et al., 1999). Treatment of developing trichomes with actin destabilizing drugs produced aberrantly expanded trichomes that phenocopied a class of trichome mutants called the *distorted* (*dis*) mutants (Feenstra, 1978; Hülskamp et al., 1994; Mathur et al., 1999; Szymanski et al., 1999). Cloning of several of the *DIS* genes showed that they encode subunits of the actin-related protein2/3 (Arp2/3) complex (Le et al., 2003; Li et al., 2003; Mathur et al., 2003a, 2003b; Saedler et al., 2004).

The Arp2/3 complex is a regulator of actin polymerization and consists of seven subunits, two of which are actin-related proteins (Arp2 and Arp3), and five other distinct proteins (ARPC1-ARPC5) (Machesky et al., 1994; Machesky and Gould, 1999). This complex has been well studied in animals, where it participates in many actin-dependent processes such as filopodia and lamellipodia formation. The Arp2/3 complex is responsible for the de novo nucleation of new actin filaments from the sides of existing actin filaments, but the complex by itself is inactive; additional factors are required to activate the complex (Pollard

[1] Current address: DNA Variation Group, Stanford Genome Technology Center, 855 California Ave., Stanford, CA 94305-8307.
[2] To whom correspondence should be addressed. E-mail doppen@botany.ufl.edu; fax 352-392-3993.
The author responsible for distribution of materials integral to the findings presented in this article in accordance with the policy described in the Instructions for Authors (www.plantcell.org) is: David G. Oppenheimer (doppen@botany.ufl.edu).
Article, publication date, and citation information can be found at www.plantcell.org/cgi/doi/10.1105/tpc.104.028670.

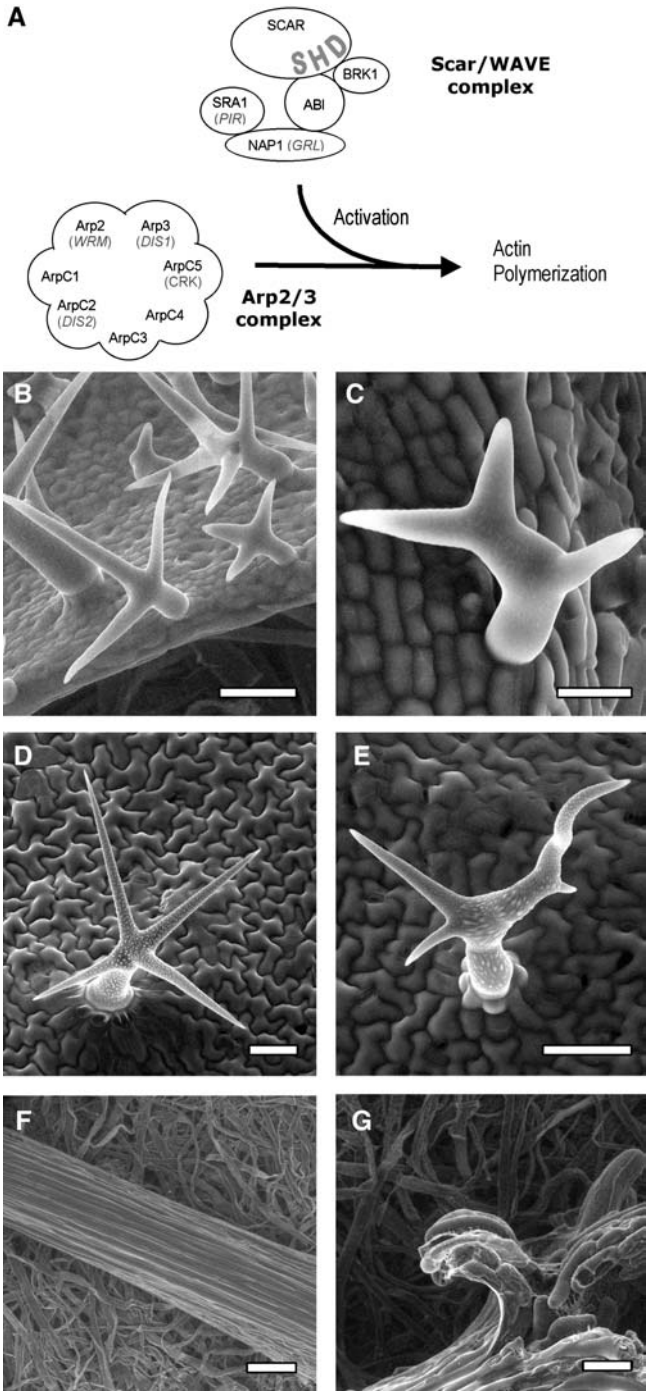

Figure 1. *itb1/scar2* Mutants Display Epidermal Cell Expansion Defects.

(A) Schematic illustration of activation of Arp2/3 complex-dependent actin polymerization. The Arabidopsis genes identified by trichome mutations are indicated below the subunit names.

(B) ESEM of developing (stage 4/5) wild-type trichomes showing even elongation of branches.

(C) ESEM of a developing *itb1-16* mutant trichome (stage 4/5) showing irregular expansion of the stalk.

(D) ESEM of a mature wild-type trichome showing symmetrical arrangement of the branches.

(E) ESEM of a mature *itb1-16* trichome showing irregular branch lengths and positions.

(F) and **(G)** ESEMs of leaf petioles of wild type **(E)** and *itb1-16* **(F)** plants. Epidermal cells on *itb1-16* mutants curl away from the subepidermal cell layers resulting in disfiguration of the petiole.

Bars = 50 μm in **(B)**, **(D)**, and **(E)**, 20 μm in **(C)**, 200 μm in **(F)**, and 100 μm in **(G)**.

and Borisy, 2003). In animals, members of the WASp (for Wiskott-Aldrich syndrome protein) and Scar/WAVE (for suppressor of cAMP receptor/WASP family verprolin-homologous protein) families are well-studied activators of the Arp2/3 complex (Weaver et al., 2003). Both WASp and Scar/WAVE proteins contain a conserved VCA (for verprolin-homology, cofilin-homology, acidic region) domain at their C termini. This domain is responsible for the binding to and activation of the Arp2/3 complex (Pollard and Borisy, 2003; Weaver et al., 2003). Whereas the activity of WASp proteins is regulated by autoinhibition, Scar/WAVE activity is regulated by binding to four additional proteins: Abi1, Nap1, PIR121, and HSPC300 (Eden et al., 2002). The most current model for Scar/WAVE activation includes binding of Abi1 to Scar/WAVE through the conserved Scar homology domain (SHD) at the N terminus of the protein (Eden et al., 2002; Innocenti et al., 2004). Signaling through the small GTPase, Rac, leads to activation and/or localization of the Scar/WAVE complex to the leading edge of lamellipodia where it activates the Arp2/3 complex and initiates actin polymerization (Innocenti et al., 2004) (Figure 1A).

In plants, all of the subunits of the Arp2/3 complex have been identified, and mutations in several of them have been characterized. Currently, all of the characterized mutants belong to a class called the *dis* mutants that show dramatic irregularities in leaf trichome shape in Arabidopsis (Hülskamp et al., 1994; Le et al., 2003; Li et al., 2003; Mathur et al., 2003a, 2003b; El-Assal Sel et al., 2004; Saedler et al., 2004). Homologs of three of the regulatory subunits of the Scar/WAVE complex also have been identified in plants. These are *BRICK1* (*BRK1*; homolog of HSPC300; Frank and Smith, 2002), *NAPP/NAP1/GNARLED* (homolog of Nap1; Brembu et al., 2004; Deeks et al., 2004; El-Assal Sel et al., 2004), and PIROGI/PIRP (homolog of PIR121; Basu et al., 2004; Brembu et al., 2004). Mutations in these Nap1 and PIR121 homologs also cause *dis* trichomes. Although no Arabidopsis *brk1* mutant has been reported, *brk1* mutants in maize (*Zea mays*) show epidermal pavement cell lobe expansion defects (Frank and Smith, 2002; Frank et al., 2003), which is another phenotype reported for the *dis* mutants (Li et al., 2003; Mathur et al., 2003a, 2003b; Brembu et al., 2004). All the Arp2/3 complex subunit mutants and the Scar/WAVE complex mutants show defects in actin organization as may be expected for mutations in regulators of actin polymerization. Thus, a large amount of circumstantial evidence suggests that the Scar/WAVE pathway for activation of the Arp2/3 complex exists in plants, but one key piece of the puzzle has been missing: a plant Scar/WAVE homolog. Recently, a family of four genes has been identified that encodes proteins distantly related at their N and C termini to the SHD and VCA domains, respectively, of Scar/WAVE proteins (Brembu et al., 2004; Deeks et al., 2004). As would be expected

for functional Scar/WAVE homologs, the VCA-like domain of one member of this family binds to G-actin in vitro (Deeks et al., 2004), and the VCA-like domains of two other members of the family activate the bovine Arp2/3 complex in vitro (Frank et al., 2005), However, evidence of an in vivo function for these proteins in activation of the Arp2/3 complex has not yet been reported.

We have been using trichome branching in Arabidopsis as a model for how directional cell expansion is modulated to produce a specific, three-dimensional shape. In a screen for mutations that affect trichome branch position, we isolated a mutant that displayed an irregular trichome branching phenotype. Positional cloning of the gene identified it as a member of the family of putative Arabidopsis Scar/WAVE homologs. Here, we report a functional analysis of this gene and show that mutations cause defects in both the actin and microtubule cytoskeletons that result in aberrant epidermal cell expansion. We also show that the SHD binds to BRK1 and that overexpression of the SHD results in a dominant negative phenotype. Our results show that the Scar/WAVE pathway for regulation of the Arp2/3 complex is functional in plants and shed light on the role of the actin cytoskeleton in plant cell shape control.

RESULTS

irregular trichome branch1 Mutants Display Cell Expansion Defects

In a screen for trichome cell shape defects, we isolated several mutants that showed defects in branch position and expansion, which we called *irregular trichome branch* (*itb*) mutants. Complementation tests and genetic mapping with molecular markers showed that these mutations are novel and represent new genes affecting trichome morphogenesis. In particular, none of these mutants mapped near any of the previously described *dis* mutants. This report focuses on one of these mutants, *itb1*. The most obvious phenotype associated with *itb1* mutations is the irregular branching pattern of the trichomes as compared with the wild type (Figures 1C and 1D). To determine the stage in trichome development during which the mutant phenotype becomes apparent, we used environmental scanning electron microscopy (ESEM) to examine developing trichomes on wild-type and *itb1* mutant leaf primordia. We found that the earliest stages of trichome development (before and including branch initiation; stages 1 to 3 after the convention of Szymanski et al., 1999) in *itb1* mutants are normal. It is shortly after branches are initiated, and the trichomes begin the rapid expansion phase, that the *itb1* trichome phenotype is apparent (Figure 1B). After the completion of branch initiation, wild-type trichome branches expand evenly, producing a symmetrical trichome containing three or four branches that converge at the top of the stalk (Figures 1A and 1C). This is in contrast with trichomes on *itb1* mutants, which expand unevenly and often produce shorter than normal branches that do not converge on a single point on the stalk (Figures 1B and 1D). In addition, the trichome stalk and branches are often twisted. To determine if branch initiation is affected in *itb1* mutants, we counted branches on mature trichomes from wild-type and *itb1* mutants. We found that there was no significant difference ($P = 0.63$, Student's *t* test) between trichome branch number on *itb1* mutants as compared with the wild type (Table 1). These results show that the *ITB1* gene is required for proper trichome expansion but is not required for proper branch initiation.

In addition to the trichome phenotype, *itb1* mutants display additional defects in cell expansion. When grown on defined media in culture, cells on the leaf petioles and hypocotyl and epidermal pavement cells on the leaves and cotyledons expand aberrantly, resulting in cells that curl out of the plane of the epidermal surface. Over time, this results in severe defects in the epidermal organization of the petioles (Figures 1E and 1F). This epidermal cell expansion phenotype is strikingly similar to that observed for the *dis* class of trichome mutants (Le et al., 2003; Mathur et al., 2003a, 2003b).

ITB1 Encodes a Plant Scar/WAVE Homolog

We used a map-based strategy to clone the *ITB1* gene. The *itb1-16* mutation was mapped relative to simple sequence length polymorphism (SSLP) markers (Bell and Ecker, 1994) to BAC clone T19C21 on chromosome 2 (Figure 2A). Because the *itb1-16* allele was isolated from a fast neutron mutagenized population, we screened BAC clone T19C21 for deletions by amplifying short regions spaced approximately every 1000 bp along the BAC clone. An ~500-bp deletion was identified in gene At2g38440 in the mutant, but the deletion was not found in the wild type. The SALK T-DNA insertion database was searched for insertions in this gene, and the resulting insertion lines (Alonso et al., 2003) were screened for plants showing the *itb1* trichome phenotype. Insertion lines SALK_039449, SALK_SALK_036491, SALK_124023, and SALK_057481 segregated plants with strong *itb1* phenotypes. Results from complementation tests showed that the insertion mutations were alleles of *itb1-16* (data not shown), which demonstrated that *ITB1* is At2g38440.

The predicted intron/exon junctions of At2g38440 were confirmed by RT-PCR. BLAST searches using the coding sequence of At2g38440 showed similarity to the N terminus of the Scar/WAVE family of Arp2/3 complex regulators (Figure 2C). The At2g38440 protein was first identified as a putative Scar homolog by Deeks et al. (2004), who named it SCAR2, and subsequently by Brembu et al. (2004), who named it WAVE4. We will follow the convention of Deeks et al. (2004), and hereafter refer to At2g38440 as *ITB1/SCAR2* (following the convention of The Arabidopsis Information Resource for gene names).

We also identified the molecular lesions in our additional alleles of *itb1* (Figure 2B). The *itb1-1* allele was identified in a T-DNA mutagenized population of Wassilewskija plants (the T-DNA did not segregate with the mutation) and contains a 7-bp deletion that leads to an in-frame stop codon and a truncated protein.

Table 1. Number of Branches on *itb1* and Wild-Type Trichomes

	Number of Trichome Branches[a]			
Genotype	2	3	4	Total[b]
itb1-16	1.7	89.7	8.6	58
Wild type	1.2	88.0	10.8	83

[a] Percentage of trichomes having the indicated number of branches.
[b] Total number of trichomes counted.

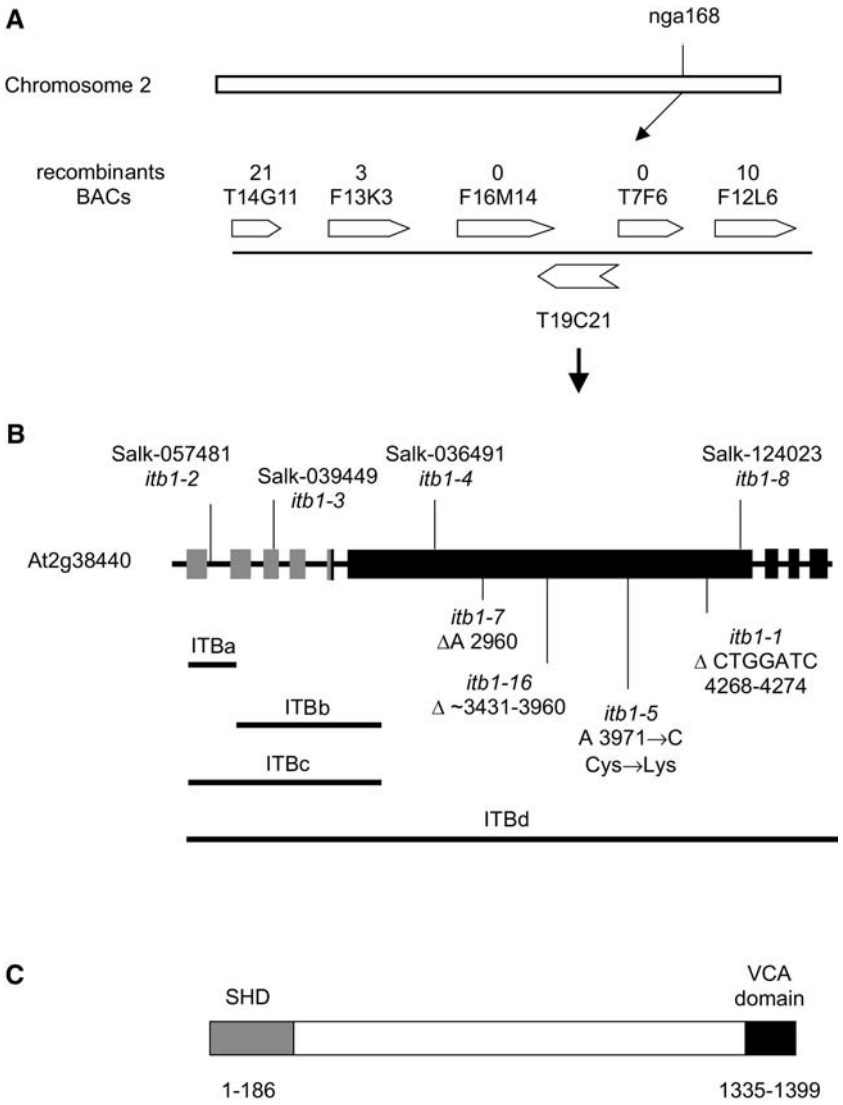

Figure 2. Positional Cloning of *ITB1*, Gene Structure of *ITB1*, Location of *itb1*/*scar2* Mutations, and Conserved Domains in the ITB1 Protein.

(A) The *itb1-16* mutation was mapped near SSLP marker nga168 on chromosome 2. Additional molecular markers were used to map the *itb1-16* mutation to BAC clone T19C21 (see Methods). The number of recombinants (out of 3660 chromatids screened) are given above BAC clones.
(B) Gene structure of *ITB1*. Thick regions represent the exons. Gray areas represent the SHD. The SALK T-DNA insertion lines are indicated above the gene model. Numbers below the gene model are the position (in base pairs, starting from the beginning of the coding sequence) of the mutations. Δ, deletion. For *itb1-16*, approximate location of the deletion is given. Thick lines under the gene model refer to regions of the coding sequence used for overexpression experiments. ITBa extends from the start codon to amino acid 73, ITBb extends from amino acid 73 to amino acid 387, ITBc extends from the start codon to amino acid 387, and ITBd extends from the start codon to the stop codon.
(C) Conserved domains in ITB1. Gray box represents the SHD, and the black box represents the VCA domain. Numbers refer to the amino acid positions comprising each domain.

Three of our *itb1* alleles were isolated from a fast neutron mutagenized population, and two of them (*itb1-7* and *itb1-16*) have deletions. The third allele, *itb1-5*, has an A-to-C transversion in the sixth exon that changes a Cys to a Lys in the ITB1/SCAR2 protein sequence. To determine the relative strength of these alleles, we examined isolated trichomes from five different *itb1* mutants. As shown in Figure 3, trichomes from all the mutants show approximately the same degree of irregularity in branching and expansion. Because the *itb1-8* mutation is near the 3′ end of the *ITB1*/*SCAR2* coding sequence, this result demonstrates that the C terminus of the ITB1/SCAR2 protein is essential for function.

ITB1 Is Expressed throughout Arabidopsis Plants, Including Leaf Primordia and Developing Trichomes

A search of Arabidopsis EST data sets identified *ITB1*/*SCAR2* ESTs from several different tissue-specific cDNA libraries. These

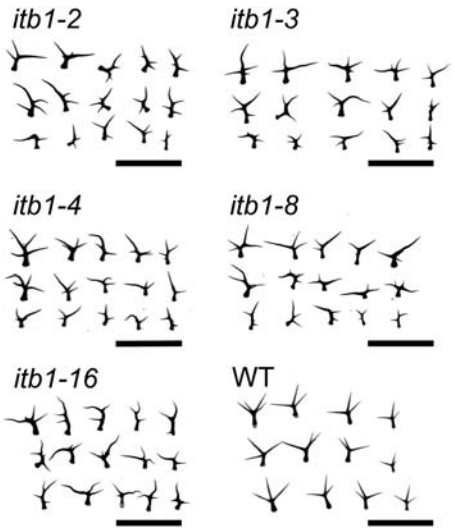

Figure 3. Evaluation of the Severity of the Trichome Phenotypes of Different *itb1/scar2* Mutants.

Trichomes from *itb1/scar2* mutants were isolated as described by Zhang and Oppenheimer (2004), stained in Toluidine blue, and photographed. The severity of the trichome phenotype is approximately the same for all the *itb1/scar2* mutants. Bars = 1 mm.

included libraries prepared from root tissue, collections of above-ground organs, developing seeds, and leaf tissue treated with bacterial pathogens. This shows that *ITB1/SCAR2* is expressed throughout Arabidopsis plants. To further examine the expression of *ITB1/SCAR2*, we performed whole mount in situ hybridization on developing leaf primordia using an *ITB1/SCAR2*-specific, antisense RNA probe. We found strong expression in developing trichomes at all stages, as well as expression throughout the leaf primordium (Figures 4A, 4C, and 4E). The patchy expression pattern observed in the leaf primordia is most likely due to incomplete penetration of the probe into the tissue. No signal was detected in the trichomes or leaf primordia subjected to hybridization with a sense strand probe (Figures 4B, 4D, and 4F). This result shows that *ITB1/SCAR2* is expressed in developing trichomes during the stages predicted by phenotypic analysis of *itb1/scar2* mutant trichomes, as well as other expanding epidermal cells.

The Actin and Microtubule Cytoskeletons Are Disorganized in *itb1/scar2* Mutants

Because the identity of the ITB1/SCAR2 protein suggested that it plays a role in the regulation of actin dynamics, we examined the actin cytoskeleton in *itb1/scar2* mutants using immunolocalization and confocal microscopy. At the earliest stages of trichome development (stages before and including branch initiation), we found no difference in actin organization between *itb1/scar2* mutants and the wild type (data not shown). Therefore, we focused our attention on stage 4/5 trichomes because the most dramatic changes in shape between the wild type and mutants occur during this stage in trichome development. In wild-type stage 4/5 trichomes, F-actin strands are visible that extend from below the branch tips into the stalk of the trichome (Figure 5A). However, in *itb1/scar2* mutants, the F-actin is arranged in thicker bundles that appear more as meshwork with fewer parallel bundles as compared with the wild type (Figure 5B). We also observed differences in the arrangement of F-actin at the cell cortex between the wild type and *itb1/scar2* mutants. In wild-type cells, transversely aligned, fine F-actin strands are observed near the branch tips. These fine F-actin filaments are arranged more randomly toward the middle of the branch and become

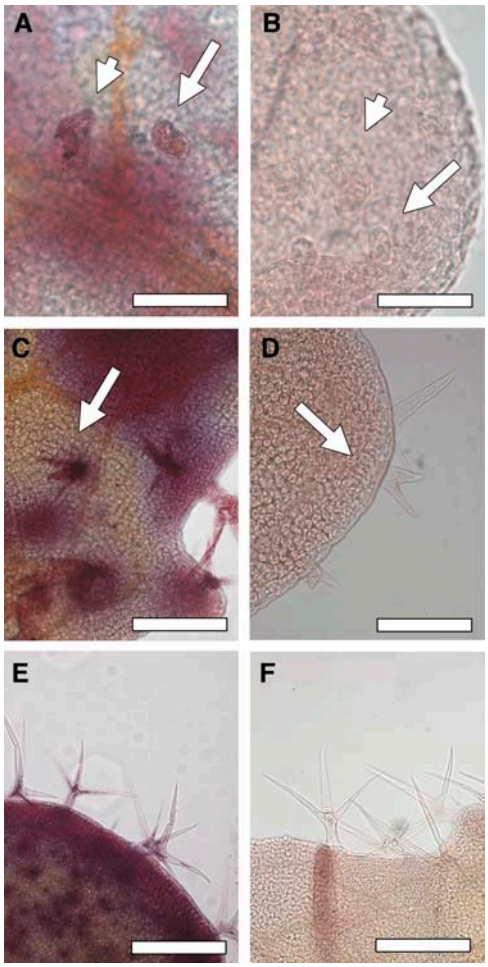

Figure 4. *ITB1/SCAR2* Is Expressed throughout Trichome Development.

(A), **(C)**, and **(E)** Light micrographs of whole mount in situ hybridization results of RLD wild-type leaf primordia hybridized to a gene-specific *ITB1/SCAR2* antisense probe.

(B), **(D)**, and **(F)** Light micrographs of whole mounts of wild-type leaf primordia hybridized to a sense-strand probe. Reddish purple color indicates hybridization of the probe to mRNA in the tissue.

Long arrows in **(A)** and **(B)** indicate incipient trichomes before branch initiation. Short arrows in **(A)** and **(B)** indicate branching trichomes. Arrows in **(C)** and **(D)** indicate branched, expanding trichomes (stage 4/5). Bars = 50 μm in **(A)** and **(B)**, 100 μm in **(C)** and **(D)**, and 200 μm in **(E)** and **(F)**.

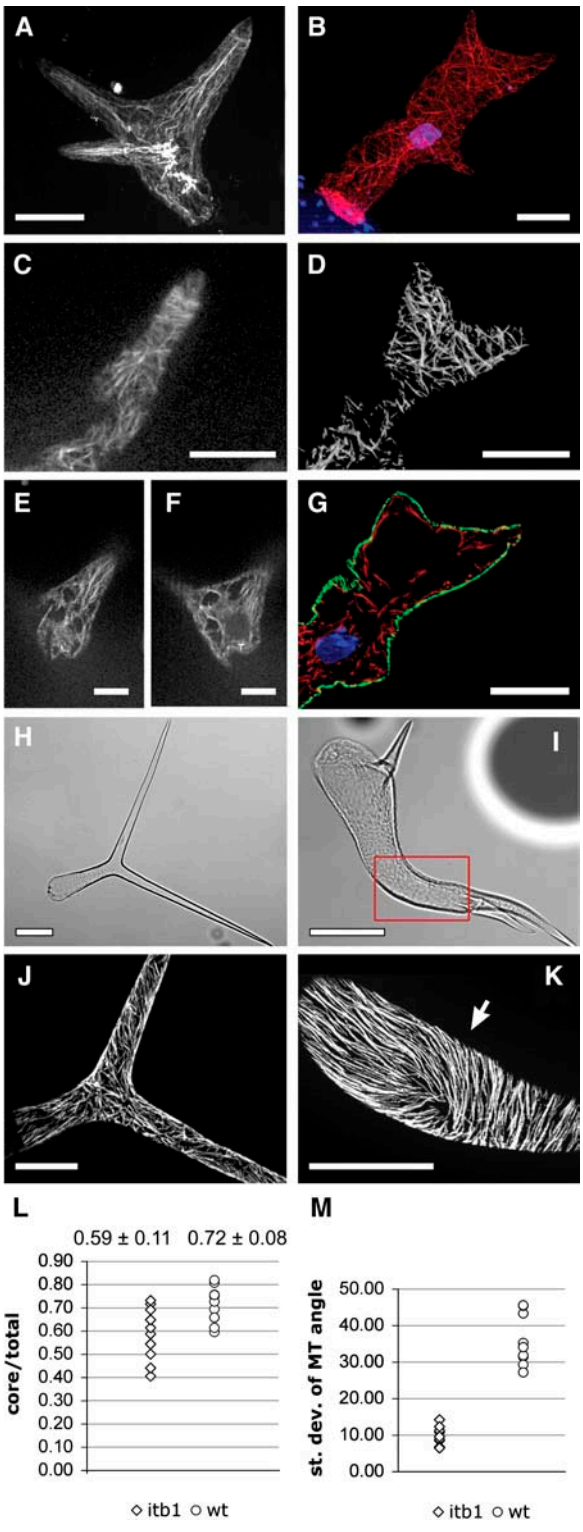

Figure 5. *itb1/scar2* Mutants Show Defects in Actin and Microtubule Cytoskeleton Organization.

Immunolocalization and fluorescent microscopy was used to visualize the actin and microtubule cytoskeletons in the wild type (**[A]**, **[C]**, **[E]**, **[F]**, and **[J]**) and *itb1/scar2-16* mutants (**[B]**, **[D]**, **[G]**, and **[K]**).

aligned parallel to the long axis of the branch near the base of the branch (Figure 5C). By contrast, we did not observe the fine, transversely aligned F-actin filaments near the branch tips in *itb1/scar2* mutants (Figure 5D). We observed almost no cortical fine actin, and the filaments appeared to be organized into thicker bundles (Figure 5D) that were more randomly arranged. We also examined the arrangement of cortical actin and subcortical or core actin in optical sections of immunofluorescently labeled trichomes. When we examined core actin organization, we found that wild-type developing trichomes have abundant core actin (Figures 5E and 5F) compared with *itb1/scar2* mutants (Figure 5G), which show less core actin, especially in the expanding trichome branches. We quantified the pixel intensity ratios of core actin filaments to total actin filaments in developing stage 4/5 trichomes. As shown in Figure 5L, the ratio of core actin/total actin is significantly less ($P < 0.0086$, Student's t test) in *itb1/scar2* mutants compared with the wild type.

We also examined the organization of the microtubule cytoskeleton in mutant and wild-type trichomes. The cortical microtubules in mature wild-type trichomes consist of short microtubule bundles with little overall alignment (Figure 5J). However, when we examined the cortical microtubule organization in mature *itb1/scar2* mutant trichomes, we found extensive, parallel arrays of microtubule bundles that generally followed the overall shape of the trichome (Figure 5K). In some instances, the parallel microtubule arrays changed orientation, but this change in direction did not correspond to an obvious topological change in the trichome, such as a branch (Figure 5K). We quantified the organization of the cortical microtubules by measuring

(A) and **(B)** Maximum projections of optical sections taken through developing (stage 4/5) wild-type **(A)** and *itb1-16* **(B)** trichomes after indirect immunofluorescent labeling of the actin cytoskeleton. In **(B)**, F-actin labeling is red, and 4′,6-diamidino-2-phenylindole (DAPI) labeling of the trichome nucleus is shown in blue.

(C) Composite image of optical sections from just below the cortical microtubules of the same trichome shown in **(A)** showing abundant fine actin and thin actin filaments.

(D) Cortical actin organization in an *itb1-16* trichome showing mostly thick actin cables.

(E) and **(F)** Single optical sections taken through the center of the trichome shown in **(A)** showing the abundant core actin.

(G) Single optical section from the center of the trichome shown in **(B)** showing the dearth of core actin in *itb1-16*. F-actin is shown in red, cortical microtubules are shown in green, and the DAPI-stained nucleus is shown in blue.

(H) and **(I)** Differential interference contrast images of mature trichomes shown in **(J)** and **(K)**. Box in **(I)** indicates region of trichome shown in **(K)**.

(J) Cortical microtubules in a mature wild-type trichome showing the generally random arrangement of short microtubule bundles.

(K) Cortical microtubules in an *itb1-16* mutant showing long, predominantly parallel microtubules. Note the change in overall orientation of the parallel microtubule bundles at arrow.

(L) Ratios of core actin signal to total actin signal in stage 4/5 branches from 10 trichomes.

(M) Standard deviations of cortical microtubule (MT) angles in branches of 10 trichomes.

Bars = 40 μm in **(A)**, **(C)**, **(D)**, **(G)**, **(J)**, and **(K)**, 20 μm in **(B)**, **(E)**, and **(F)**, and 100 μm in **(H)** and **(I)**.

the angle between an imaginary line and all intersecting microtubule bundles in maximum projections of *itb1/scar2* and wild-type trichomes. The standard deviation from the mean microtubule angle was used as a measure of the degree of parallelism of the microtubules. As shown in Figure 5M, the cortical microtubules in *itb1/scar2* trichomes had a significantly more parallel arrangement as compared with wild-type cortical microtubules ($P < 10^{-6}$). These results show that defects in ITB1/SCAR2 lead to organizational defects in both the actin and microtubule cytoskeletons.

Overexpression of the SHD of ITB1/SCAR2 Causes Abnormal Trichome Expansion

To gain insight into the function of *ITB1/SCAR2* in trichome development, we fused various subfragments of the N-terminal 388 amino acids of ITB1/SCAR2 with green fluorescent protein (GFP). We expressed the fusions from the *Cauliflower mosaic virus* 35S RNA promoter (35S) and the *GL2* promoter (Szymanski et al., 1998) in both wild-type and *itb1/scar2* mutant plants. The ITBa and ITBb fusions lack a complete SHD, and the ITBc fusion retains a complete SHD (Figure 2B). The trichome phenotype was examined in at least 20 independent transformed lines for each construct. Wild-type or *itb1-16* mutants that expressed either ITB1a or ITB1b did not show any alteration in trichome phenotype. However, when *itb1-16* plants were transformed with an ITB1c, the fragment encoding an intact SHD, the trichome phenotype became more severe (Figures 6A to 6F). Similarly, when ITB1c was used to transform wild-type plants, a dominant negative phenotype was observed (Figures 6G to 6L). Because ITB1a and ITB1b (both of which lacked an intact SHD) did not cause an altered trichome phenotype, it is unlikely that the altered trichome phenotype is due to cosuppression. We also noted that the 35S promoter caused a more severe trichome phenotype than the *GL2* promoter when used to express the ITBc fusion in *itb1-16* mutants (cf. Figures 6B and 6E with 6C and 6F). The trichomes produced on *itb1-16* mutants transformed with 35S-ITBc were small and twisted with very little branch expansion (Figures 6B and 6E). However, in wild-type plants, the *GL2* promoter consistently produced a stronger trichome phenotype compared with the 35S promoter. Wild-type plants transformed with 35S-ITBc produced trichomes similar in appearance to those on untransformed *itb1-16* mutants (cf. Figures 6A and 6D with 6H and 6K). By contrast, wild-type plants transformed with GL2-ITBc produced trichomes that were generally more twisted and with less branch expansion than the trichomes on 35S-ITBc transformants (Figures 6I and 6L). The reason for this phenotypic difference between the two promoters in the different backgrounds is unclear. The main difference between the two promoters is that the *GL2* promoter is strongly expressed in developing and mature trichomes and at the base of leaf primordia (Szymanski et al., 1998), whereas expression from the 35S promoter is found throughout the leaf primordia as well as the trichomes (Larkin et al., 1994). No obvious dominant negative effects on epidermal pavement cell morphology were observed in any of the transformants (data not shown).

To confirm that the GFP moiety was not responsible for the observed trichome phenotypes, we transformed *itb1-16* mutants with the full-length *ITB1/scar2* coding sequence expressed from the 35S promoter. This construct was able to rescue the *itb1* phenotype as shown in Figures 6M and 6P. In addition, when we transformed *itb1-16* mutants with 35S-ITBc constructs lacking GFP, we found that the transformants still produced the more severe trichome phenotype (Figures 6N and 6Q). Similarly, when wild-type plants were transformed with the 35S-ITBc construct lacking GFP, trichomes on the transformants showed the same irregular trichome phenotype as wild-type transformants containing the 35S-ITBc construct containing the GFP fusion (cf. Figures 6H and 6K with 6O and 6R).

The SHD of *ITB1/SCAR2* Binds to BRK1 in Vitro

WAVE1 protein isolated from bovine brain extracts was found to be associated with HSPC300 (Eden et al., 2002), and a direct binding interaction between WAVE2 and HSPC300 has been demonstrated in vitro (Gautreau et al., 2004). Moreover, two members of the Arabidopsis Scar/WAVE family, SCAR1 and SCAR3, have been shown to bind in vitro to the Arabidopsis HSPC300 homolog, BRK1, via their SHDs (Frank et al., 2005). These observations suggested that the dominant negative effect of overexpressing the SHD of ITB1/SCAR2 might be due to its binding of BRK1 in vivo. To investigate this possibility, we tested whether BRK1 could bind to the SHD of ITB1/SCAR2 or to a fragment of ITB1/SCAR2 lacking the SHD. T7-tagged BRK1 was cotranslated in vitro with various portions of the ITB1/SCAR2 coding sequence and collected by binding to anti-T7 antibody-conjugated agarose beads. Bound proteins were analyzed by SDS-PAGE followed by autoradiography. As expected, we found that BRK1 bound to the SHD of ITB1/SCAR2 (Figure 7, lanes 7 and 8; note presence of ITB SHD band in lane 8). However, BRK1 did not bind to an 1106–amino acid fragment that did not contain the SHD (Figure 7, lanes 5 and 6; note absence of ITBΔSHD band in lane 4). This result shows that the SHD of ITB1/SCAR2 is both necessary and sufficient for binding to BRK1.

DISCUSSION

The Scar/WAVE Pathway for Arp2/3 Activation Is Conserved in Plants

Mutations disrupting the Arp2/3 complex in Arabidopsis produce trichome shape defects and subtle changes in epidermal pavement cell shape, indicating a critical role for Arp2/3-dependent actin polymerization in epidermal cell shape control (Le et al., 2003; Li et al., 2003; Mathur et al., 2003a, 2003b; El-Assal Sel et al., 2004; Saedler et al., 2004). Similar distorted trichome phenotypes result from mutations in the *GRL* and *PIR* genes, encoding Arabidopsis homologs of Nap1 and PIR121, respectively (Basu et al., 2004; Brembu et al., 2004; Deeks et al., 2004; El-Assal Sel et al., 2004). Nap1 and PIR121 are components of a complex associated with animal WAVE proteins that functions to regulate the activity and/or localization of Scar/WAVE (Innocenti et al., 2004; Steffen et al., 2004). Thus, evidence has emerged that the Scar/WAVE regulatory complex is conserved in plants and plays an essential role in activation of the Arp2/3

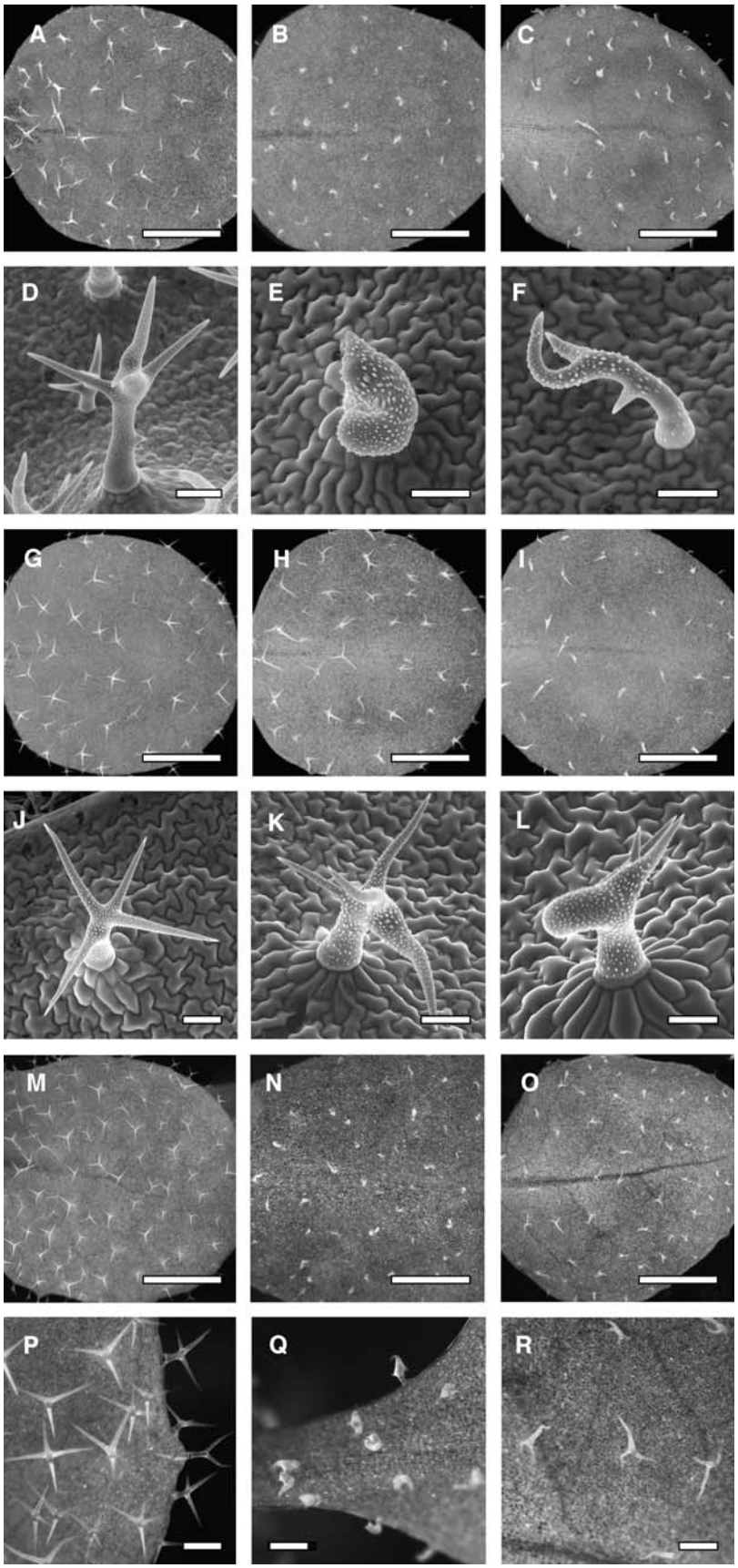

Figure 6. Overexpression of the SHD of ITB1/SCAR2 Causes a Dominant Negative Trichome Phenotype.

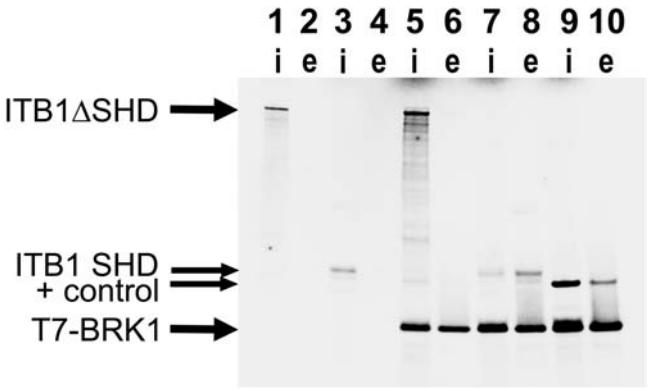

Figure 7. The SHD of ITB1/SCAR2 Binds to BRK1 in Vitro.

T7 tag pull-down assays were performed on T7-tagged BRK1 protein translated in the presence of either the SHD of ITB1-SHD or ITB1ΔSHD, which lacked the SHD. Proteins bound to anti-T7 antibody-conjugated agarose beads were visualized by autoradiography after separation by SDS-PAGE. For each experiment, a sample of the input (i) proteins and the proteins eluted (e) from the beads was analyzed. Lane 1, input sample 1 containing amino acids 212 to 1317 of ITB1/SCAR2, which lacks the SHD (ITB1ΔSHD). Lane 2, bound proteins from sample 1. Lane 3, input sample 2 containing the SHD of ITB1/SCAR2 (ITB1 SHD). Lane 4, bound proteins from sample 2. Lane 5, input sample 3 containing T7-tagged BRK1 and amino acids 212 to 1317 of ITB1/SCAR2, which lacks the SHD (ITB1ΔSHD). Lane 6, bound proteins from sample 3. Lane 7, input sample 4 containing T7-tagged BRK1 (T7-BRK1) and the SHD of ITB1/SCAR2 (ITB1 SHD). Lane 8, bound proteins from sample 4. Lane 9, input sample 5 containing T7-tagged BRK1 and the SHD of SCAR1 (+ control), which was previously shown to bind to BRK1 (Frank et al., 2005). Lane 10, bound proteins from sample 5.

complex. However, the identity of the Arp2/3 activator within this putative complex has remained elusive. We provide strong evidence that ITB1/SCAR2 is a Scar/WAVE homolog that functions in association with GRL, PIR, and BRK1 to positively regulate the Arp2/3 complex.

ITB1 encodes SCAR2, which belongs to a family of four proteins in Arabidopsis recently identified as candidates for Scar/WAVE homologs on the basis of weak sequence homology to Scar/WAVE proteins (Brembu et al., 2004; Deeks et al., 2004). The C-terminal VCA-like domains of two other members of this family, SCAR1 and SCAR3, have been shown to activate the bovine Arp2/3 complex in vitro (Frank et al., 2005). We show that mutations in ITB1/SCAR2 cause the same alterations in cytoskeletal organization and the same syndrome of cell expansion defects as do mutations disrupting the Arp2/3 complex, PIR, and GRL. Therefore, the phenotype of *itb1/scar2* mutants is consistent with an essential role for ITB1/SCAR2 in activation of the Arp2/3 complex through association with GRL and PIR. All the *itb1/scar2* alleles we examined show essentially the same irregular trichome phenotype. This result is not unexpected because all the alleles have lesions upstream of the C-terminal VCA domain, which is essential for binding to and activation of the Arp2/3 complex, and hence for function. Because *ITB1/SCAR2* is one of four members of a gene family, it is perhaps surprising that the *itb1/SCAR2* mutant trichome shape defect is almost as severe as that resulting from disruption of the Arp2/3 complex itself. Thus, *ITB1/SCAR2* is not functionally redundant with other members of the SCAR family, which may function primarily in Arp2/3-dependent processes other than regulation of trichome expansion.

Interestingly, ITB1/SCAR2 lacks a Pro-rich region like that found in other SCAR family members. The longest region of multiple Pro residues in ITB1/SCAR2 is **PP**N**P**EDM**P** **P**L**PP** (amino acids 1053 to 1064), whereas the Pro-rich region of human Scar1 contains stretches of PPPPPPPLP, PPPPVP-PPPPPP, and PPPPPPPPLPPP as well as additional Pro-rich regions longer that that found in ITB1/SCAR2. In animal Scar proteins, the G-actin binding protein, profilin, has been shown to bind to the polyproline region, but its role is not understood (Higgs and Pollard, 1999; Oda et al., 2004). The lack of a well-defined polyproline region in ITB1/SCAR2 suggests that profilin's role is performed by additional as yet undiscovered proteins or that other profilin binding sites exist in ITB1/SCAR2.

The *ITB1/SCAR2* Expression Pattern Is Consistent with Its Role in Cell Expansion

The detection of *ITB1/SCAR2* expression in all cell types of developing leaf primordia is consistent with the phenotype exhibited by *itb1/scar2* mutants. Defects in expansion of petiole epidermal cells and trichomes are readily apparent in *itb1/scar2* mutants. The epidermal cell type most obviously affected is the trichome. We detected *ITB1/SCAR2* expression in trichomes at

Figure 6. (continued).

Light micrographs of leaves (**[A]** to **[C]**, **[G]**, **[H]**, and **[M]** to **[R]**) and ESEMs of trichomes (**[D]** and **[E]** and **[J]** to **[L]**).
(A) and **(D)** *itb1-16* trichome phenotype showing typical irregular trichome branching.
(B) and **(E)** *itb1-16* transformed with 35S-ITBc, showing a severe distorted phenotype.
(C) and **(F)** *itb1-16* transformed with GL2-ITBc showing a more severe trichome phenotype than *itb1-16* alone but less severe than the trichomes on 35S-ITBc transformants.
(G) and **(J)** RLD wild type showing normal trichome shape.
(H) and **(K)** RLD wild type transformed with 35S-ITBc showing irregularly shaped trichomes.
(I) and **(L)** RLD wild type transformed with 35S-ITBc showing a more severe phenotype than 35S-ITBc transformants.
(M) and **(P)** *itb1-16* transformed with 35S-ITBd (lacking the GFP fusion) showing wild-type trichome shape.
(N) and **(Q)** *itb1-16* transformed with 35S-ITBc (lacking the GFP fusion) showing a severe distorted trichome phenotype.
(O) and **(R)** RLD wild type transformed with 35S-ITBc (lacking the GFP fusion) showing irregularly shaped trichomes.
Bars = 1 mm in **(A)** to **(C)**, **(G)** to **(I)**, and **(M)** to **(O)**, 50 μm in **(D)** to **(F)** and **(J)** to **(N)**, and 100 μm in **(P)** to **(R)**.

the earliest stages of development, including before branch initiation even though a phenotype at these early stages of development is not apparent. In addition, expression of *ITB1/SCAR2* was also detected in mature trichomes that had ceased expansion (Figure 4E). This suggests that Arp2/3 complex activation may play a role in trichomes beyond controlling cell expansion.

ITB1/SCAR2 Is Required for Proper Organization of the Actin and Microtubule Cytoskeletons

Mutations in components of the Arp2/3 complex and the putative Scar/WAVE regulatory complex all show defects in actin organization (Frank and Smith, 2002; Le et al., 2003; Li et al., 2003; Mathur et al., 2003a, 2003b; Basu et al., 2004; Brembu et al., 2004; Deeks et al., 2004; El-Assal Sel et al., 2004; Saedler et al., 2004). In addition, we demonstrated in this report that mutations in ITB1/SCAR2 also lead to defects in trichome actin organization. This is consistent with their likely roles as regulators of actin filament initiation and branching. However, the connection between actin polymerization and control of directional cell expansion remains unclear. Although all of the above-mentioned mutants have distorted trichomes, the trichomes are still able to expand anisotropically. This demonstrates that there is still significant control in the direction of cell expansion despite the lack of Arp2/3 complex-derived actin networks in these mutants.

In addition to the defects in actin organization, we documented cortical microtubule defects in *itb1/scar2* mutants. A cortical microtubule defect also has been reported for the *dis* mutant, *dis2*, that encodes the ARP2C subunit of the Arp2/3 complex (Schwab et al., 2003; Saedler et al., 2004). One possible explanation for the cortical microtubule defect is that the cortical microtubule bundles passively follow the contours of the aberrantly expanding trichome cell in *itb1/scar2* mutants. However, this does not account for cases where the cortical microtubule orientation does not correspond to a topological change in the trichome (see Figure 5F). Also, it does not account for the apparent increase in length of the cortical microtubule bundles (Schwab et al., 2003; Figures 5E and 5F). This difference in cortical microtubule bundle length suggests that cortical microtubule dynamics are altered in the mutant as well.

Currently, we are unable to distinguish direct from indirect effects of altered Arp2/3 activity on cortical microtubule organization/dynamics, but future study will help clarify the relationship between actin nucleation and microtubule organization.

In Vivo ITB1/SCAR2 Function Requires Additional Factors and Is Partially Redundant in Trichome Cells

The dominant negative effect of overexpression of the SHD of ITB1/SCAR2 in wild-type plants strongly suggests that additional factors are required for SCAR function, further supporting the notion that ITB1/SCAR2 functions as a component of the conserved Scar/WAVE regulatory complex (Figure 1A). Because the ITBc construct lacked the VCA domain, which is required for Arp2/3 complex activation (Pollard and Borisy, 2003), any factors bound to ITBc would be prevented from binding to the endogenous SCARs present in developing trichomes. This would inhibit proper Arp2/3 complex activation and produce a *dis* trichome phenotype, which is what was observed. Several possibilities exist for binding partners of ITB1/SCAR2. First, it has been shown that binding of Abi1 to the SHD of WAVE2 is essential for in vivo function (Innocenti et al., 2004). Predicted Arabidopsis genes encoding proteins with weak homology to Abi1 have been identified (Deeks et al., 2004) and are thus candidates for binding to the SHD of ITB1/SCAR2. Second, we have shown here that BRK1 binds to the SHD of ITB1/SCAR2. Moreover, we show that the SHD of ITB1/SCAR2 is necessary for BRK1 binding because a deletion of ITB1/SCAR2 lacking the SHD fails to bind to BRK1. Although the role of HSPC300 in activating the Arp2/3 complex remains to be elucidated, in vivo and in vitro association of HSPC300 with WAVE is well documented (Eden et al., 2002; Gautreau et al., 2004; Innocenti et al., 2004).

Importantly, Abi1 binding to the SHD was shown to mediate the assembly and proper localization of the WAVE-Abi1-Nap1-PIR121 complex (Innocenti et al., 2004; Steffen et al., 2004). Homologs of the other known members of the Scar/WAVE regulatory complex have been identified in Arabidopsis (Frank and Smith, 2002; Basu et al., 2004; Brembu et al., 2004; Deeks et al., 2004; El-Assal Sel et al., 2004). In addition, interactions between the PIR121 homolog (*PIROGI*/*PIRP*) and the Nap1

Table 2. SSLP Markers Used for Mapping the *ITB1* Gene

Name	Sequence (5′→3′)	SSLP Length				Location (BAC)
		Col	RLD	L*er*	Ws	
S1 F S1 R	TTTGGATGGATTTGTGCGTG CGATGAGGTCAATCCTAAAGATCAG	81	81	69	81	T14G11
S2 F S2 R	GACATTGGCTCTTTCTACGATTTC TGCGTGCATGTAATATCTTATCAG	129	167	177	187	F13K3
S3 F S3 R	CCACGGCCAGGTAATGTTTTAA CAGTGTAGTGATCTTTATAATGTGATGA	78	78	94	78	F16M14
S4 F S4 R	TAGAGATTGGACCCACAAGAGA CGCTTCGACTCACAAATATTTTATG	178	178	178	135	T7F6
S5 F S5 R	CGCTTCGACTCACAAATATTTTATG TTGAAAGATCACGCCGGCGA	150	150	120	120	F12I6

L*er*, Landsberg *erecta*; Ws, Wassilewskija.

homolog (NAP1/NAPP) have been documented (Basu et al., 2004; El-Assal Sel et al., 2004). If the Arabidopsis Scar/WAVE complex behaves similarly to that in animal cells, then overexpression of the SHD would recruit these other factors into a nonfunctional complex through interactions with ABI.

There are several explanations for the inability to detect GFP fluorescence of the ITBc proteins in the trichomes of transgenic plants. First, there may be posttranscriptional regulation of ITB1 abundance. This is suggested by the observation that in animal cells, deletion or RNA interference depletion of PIR121 or Nap1 results in dramatic reduction of Scar/WAVE protein levels, indicating that Scar/WAVE protein not associated with PIR121 and Nap1 is rapidly degraded (Blagg et al., 2003; Kunda et al., 2003; Rogers et al., 2003). Second, the conformation of the fusion protein may be such that GFP cannot fold correctly.

In conclusion, our data support the hypothesis that activity of the Arp2/3 complex is regulated through a conserved pathway involving the Scar/WAVE homolog ITB1/SCAR2 and the HSPC300 homolog BRK1. Loss of function of ITB1/SCAR2 leads to actin and microtubule defects, suggesting a close interrelationship between the two cytoskeletons during cell expansion. The dominant negative effects of overexpression of the SHD, along with localization of this domain in trichome branch tips, supports the idea that assembly and localization of a multiprotein, ITB1/SCAR2-containing complex is essential for proper epidermal cell expansion. These results provide key insight into the regulation of the Arp2/3 complex in plants and its role in cytoskeletal organization during directional cell expansion.

METHODS

Plant Growth Conditions

Arabidopsis thaliana wild-type and *itb1/scar2* mutants were grown in Fafard 2 Mix (Conrad Fafard, Agawam, MA). Plants were grown at room temperature under continuous light from 40-W fluorescent tubes and fertilized twice during their growth cycle with PGP nutrient solution (Pollock and Oppenheimer, 1999). All mutant alleles were backcrossed at least once before analysis. To examine the root and epidermal cell phenotypes of *itb1/scar2* mutants, plants were grown on MS medium with 1% sucrose solidified with 7 g/L agar. The plates were sealed with Parafilm (American National Can, Neenah, WI) and incubated in a growth chamber at 25°C with 8 h of light per day.

Genetic Mapping

Rschew (RLD) *itb1-16* mutants were crossed to Landsberg *erecta*, Columbia (Col) wild type, and Wassilewskija wild type to generate mapping populations. A total of 1830 phenotypically *itb1/scar2* plants were selected from the F2 populations. Once the seedlings had initiated the second leaf pair, one of the cotyledons from each mutant plant was removed for DNA extraction with the RED Extract-N-Amp plant PCR kit (Sigma-Aldrich, St. Louis, MO). The isolated DNA was used to map the *itb1/scar2* mutation relative to SSLPs. The primer pairs used for the mapping and the SSLPs identified are listed in Table 2.

Immunolocalization and Quantification of Actin and Microtubule Defects

To label the developing trichomes on leaf primordia, we essentially followed the procedure described by Sugimoto et al. (2000), except that the pectinase Y-23 was replaced by a solution that contained 1% Driselase and 0.5% Pectinase (Sigma-Aldrich), and the enzyme treatment step was extended to 2 h. Also, 0.05% Triton X-100 was included in the fixation and subsequent steps as a wetting agent. Mature trichomes were labeled as previously described (Zhang and Oppenheimer, 2004). Monoclonal anti-actin antibody clone C4 (ICN Biochemicals, Irvine, CA) was used at a 1:400 dilution to localize the actin cytoskeleton, and monoclonal anti-α-tubulin clone B-5-1-2 (Sigma-Aldrich) was used at a 1:1000 dilution for localization of the microtubule cytoskeleton. Fluorescein isothiocyanate–conjugated goat anti-mouse IgG secondary antibody (Sigma-Aldrich) was used at a 1:100 dilution to detect the primary antibodies. For labeling both the actin and microtubule cytoskeletons, monoclonal mouse anti-α-tubulin Ab-2 (clone DM1A) IgG_1/κ (Lab Vision, Fremont, CA) was used at a 1:250 dilution, and monoclonal mouse anti-actin clone JLA20 IgM (Oncogene Research Products, Boston, MA) was used at a 1:200 dilution. Cy3-conjugated goat anti-mouse IgM secondary antibody (Jackson Immunochemicals, West Grove, PA) was used at a 1:250 dilution to detect the anti-actin primary antibody, and Alexafluor 488-conjugated goat anti-mouse IgG secondary antibody (Molecular Probes, Eugene, OR) was used at a 1:250 dilution to detect the microtubule cytoskeleton. Trichome nuclei were localized by staining for several minutes in 5 μg/mL of DAPI.

To quantify actin filament organization in developing trichomes, the method described by Le et al. (2003) was used, except that the cortical region was defined as extending 2.0 μm from the edge of the cell toward the cell interior. Total integrated fluorescence intensity measurements were obtained for single trichome branches from 10 stage 4/5 developing trichomes.

To quantify cortical microtubule organization, microtubules were immunolocalized as described above, optical sections were collected, and maximum projections were prepared. For a given projection, a 20-μm line was drawn approximately transverse to the long axis of the trichome at a position immediately distal to a trichome branch point. The angle between this line and each of the intersecting microtubule bundles (typically 17) was measured, and the standard deviation of the collection of angles was used as a measure of the degree of parallelism of the cortical microtubules. Ten trichomes were analyzed for each genotype.

Microscopy

Fluorescent images were collected with a Zeiss Axiocam HRm camera mounted on a Zeiss Axioplan 2 Imaging microscope (Jena, Germany). The following filter sets were used to collect fluorescent images: red fluorescence was obtained with Zeiss filter set 20 (excitation, 546/12; dichroic, 560 LP; emission, 575 to 640), green fluorescence was obtained with Zeiss filter set 10 (excitation, 450 to 490; dichroic, 510 LP; emission, 515 to 565), and DAPI fluorescence was obtained with Zeiss filter set 02 (excitation, 365; dichroic, 395 LP; emission, 420 LP). Optical sections were collected using the Zeiss Apotome and Axiovision 4.1 software. Light micrographs were collected with a Zeiss Axiocam MRc5 camera mounted on a Zeiss Stemi SV11 dissecting microscope. For ESEM, fresh plant tissue was placed on a moist paper towel and placed in an Electroscan Model E-3 environmental scanning electron microscope. Samples were scanned at 20 kV under 1 to 2 torr pressure.

Molecular Techniques

Total RNA from 6-week-old Col wild-type plants was isolated using the RNeasy plant mini kit (Qiagen, Valencia, CA) according to the manufacturer's instructions. First-strand cDNA synthesis was primed using oligo$(dT)_{20}$. The cDNA was amplified by RT-PCR. The amplification was done according to the protocol provided with the cMaster RT plus PCR system (Eppendorf, Hamburg, Germany). Genomic DNA was

extracted using the DNeasy plant mini kit (Qiagen). To identify the *itb1/scar2* mutations, PCR was used to amplify the coding region of *ITB1* from the genomic DNA of different *itb1/scar2* mutants. All PCR products were sequenced by the Interdisciplinary Center for Biotechnology Research at the University of Florida.

For overexpression of *ITB1*, various regions of the *ITB1*/*SCAR2* genomic sequence (ITBa, ITBb, ITBc, and ITBd; see Figure 2) were amplified by PCR using primer pairs that introduced *Nco*I sites at both ends of the PCR products. ITBa encodes amino acids 1 to 73, ITBb encodes amino acids 73 to 387, ITBc encodes amino acids 1 to 387, and ITBd encodes the full-length ITB1 coding sequence. The PCR products representing ITBa, ITBb, and ITBc were cloned into the *Nco*I site of the GFP fusion vector, pAVA319 (von Arnim et al., 1998), resulting in GFP fusions to the C termini of the ITBa, ITBb, and ITBc coding regions. The resulting gene fusions were liberated by digestion with *Xho*I and *Pst*I and transferred to either *Xho*I-*Pst*I digested pAM-PAT-GW (Bekir Ulker, Max Planck Institute for Plant Breeding, Cologne, Germany) for expression from the 35S promoter or pCK86 (Arp Schnittger, Max Planck Institute for Plant Breeding) for expression from the GL2 promoter. To produce constructs that lacked GFP, the 35S:ITBc-GFP construct was digested with *Nde*I and *Hin*dIII to liberate the GFP moiety, which was then replaced with *Nde*I-*Hin*dIII fragments containing either the remaining ITB1 coding sequence (to generate ITBd) or the remainder of the ITBc region (to generate ITBc lacking GFP). The resulting constructs were used to transform *Agrobacterium tumefaciens* strain GV3101, which was subsequently used to transform Arabidopsis RLD wild-type and RLD *itb1-16* mutant plants by the vacuum infiltration method (Bechtold et al., 1993). Transgenic plants were selected by spraying the T1 seedlings with 0.1% Finale (Farnam Companies, Phoenix, AZ) three times (at 2-d intervals) starting when the first leaf pair had completely expanded.

In Situ Hybridization

Fixation, dehydration, and clearing of young leaf primordia were performed essentially as described by Jackson (1991) except that Histoclear (National Diagnostics, Atlanta, GA) was used instead of xylene. The tissue was processed through 100% Histoclear and then back through the histoclear/ethanol series, rehydrated through an ethanol series, and stored in PBS. RNA probes were made using the DIG RNA labeling kit (Roche Diagnostics, Indianapolis, IN) following the manufacturer's instructions. ITB1-specific primer pairs were designed such that a T7 promoter was introduced, and the transcription template was prepared by PCR. The ITB1-specific antisense primers were as follows (the T7 promoter sequence is given in lowercase letters): ITB1-ist-F, 5′-CGATCCTGAAGAACGTGATGGTCG-3′; ITB1-ist-R, 5′-taatacgactcactatagggAAACTTCCATCCCCACCCCAGCT-3′. The ITB1 sense control primers were as follows: ITB1-ist-cF, 5′-taatacgactcactatagggTGCCGTTGACGAGGTACCAATCTC-3′; ITB1-ist-cR, 5′CATCTCAGCAGCAAACTCAGCGAG-3′. The in situ hybridization and detection steps were performed essentially as described by Drews et al. (1991), except that times for prehybridization and hybridization with the RNA probe were extended to overnight and 24 h, respectively.

In Vitro ITB1 Binding Assays

Plasmid SK600 contained a segment of the coding sequence of ITB1/SCAR2 encoding the SHD (amino acids 1 to 199) in pBluescript II SK+. Plasmid SK3135 contained a segment of the coding sequence of ITB1/SCAR2 encoding amino acids 212 to 1317 in pBluescript II SK+. The SHD of SCAR1 and T7-BRK1 in pET28 were generated as described by Frank et al. (2005). The SHD of SCAR1 was previously shown to bind to BRK1 protein in vitro and was used in this assay as a positive control (+ control). For in vitro transcription/translation experiments, plasmids were linearized and purified using phenol/chloroform extraction followed by ethanol precipitation. Pairs of DNA plasmids (SK600, SK3135 or + control plus T7-BRK1) were cotranscribed and cotranslated in vitro using the TNT T7 wheat germ extract system (Promega, Madison, WI) according to the manufacturer's protocols. Each 50-μL reaction contained 0.1 to 0.2 μg of each DNA template and 40 μCi L-[^{35}S] Met (Amersham Biosciences, Piscataway, NJ; 10 mCi/mL). After a 90-min incubation at 30°C, the reactions were diluted fourfold with PBS supplemented with 1 mM DTT and 1/100 protease inhibitor cocktail for plant cell and tissue extracts (Sigma-Aldrich). A 25-μL sample of anti-T7 Tag antibody agarose (Novagen, San Diego, CA) was added to each reaction and incubated at 4°C for 1 h with end-over-end rotation. The anti-T7 Tag antibody agarose beads were washed twice with 1 mL of PBS and then boiled in SDS loading buffer. Samples were separated by electrophoresis on a NuPage Novex Bis-Tris gel (4 to 12%; Invitrogen, Carlsbad, CA) using Mes SDS running buffer. After fixation and drying of gels, protein bands were detected using a PhosphorImager (Molecular Dynamics, Boston, MA).

ACKNOWLEDGMENTS

The authors wish to thank Robert Goddard for help with the ESEMs and members of the authors' laboratories for helpful discussions and critical reading of the manuscript. The authors gratefully acknowledge the ABRC for supplying the SALK T-DNA insertion lines. This work was supported by National Science Foundation Grant IBN-0091393 (to D.G.O.) and National Science Foundation Grant IBN-0212724 (to L.G.S.).

Received October 18, 2004; revised May 25, 2005; accepted May 26, 2005; published July 8, 2005.

REFERENCES

Abe, T., Thitamadee, S., and Hashimoto, T. (2004). Microtubule defects and cell morphogenesis in the lefty1 lefty2 tubulin mutant of *Arabidopsis thaliana*. Plant Cell Physiol. **45,** 211–220.

Alonso, J.M., et al. (2003). Genome-wide insertional mutagenesis of *Arabidopsis thaliana*. Science **301,** 653–657.

Basu, D., El-Assal Sel, D., Le, J., Mallery, E.L., and Szymanski, D.B. (2004). Interchangeable functions of Arabidopsis PIROGI and the human WAVE complex subunit SRA1 during leaf epidermal development. Development **131,** 4345–4355.

Bechtold, N., Ellis, J., and Pelletier, G. (1993). *In planta Agrobacterium* mediated gene transfer by infiltration of adult *Arabidopsis thaliana* plants. C. R. Acad. Sci. III, Sci. Vie **316,** 1194–1199.

Bell, C.J., and Ecker, J.R. (1994). Assignment of 30 microsatellite loci to the linkage map of *Arabidopsis*. Genomics **19,** 137–144.

Blagg, S.L., Stewart, M., Sambles, C., and Insall, R.H. (2003). PIR121 regulates pseudopod dynamics and SCAR activity in Dictyostelium. Curr. Biol. **13,** 1480–1487.

Brembu, T., Winge, P., Seem, M., and Bones, A.M. (2004). NAPP and PIRP encode subunits of a putative wave regulatory protein complex involved in plant cell morphogenesis. Plant Cell **16,** 2335–2349.

Burk, D.H., Liu, B., Zhong, R., Morrison, W.H., and Ye, Z.H. (2001). A katanin-like protein regulates normal cell wall biosynthesis and cell elongation. Plant Cell **13,** 807–828.

Deeks, M.J., Kaloriti, D., Davies, B., Malho, R., and Hussey, P.J. (2004). Arabidopsis NAP1 is essential for Arp2/3-dependent trichome morphogenesis. Curr. Biol. **14,** 1410–1414.

Drews, G.N., Bowman, J.L., and Meyerowitz, E.M. (1991). Negative regulation of the Arabidopsis homeotic gene AGAMOUS by the APETALA2 product. Cell **65,** 991–1002.

Eden, S., Rohatgi, R., Podtelejnikov, A.V., Mann, M., and Kirschner,

M.W. (2002). Mechanism of regulation of WAVE1-induced actin nucleation by Rac1 and Nck. Nature **418,** 790–793.

El-Assal Sel, D., Le, J., Basu, D., Mallery, E.L., and Szymanski, D.B. (2004). Arabidopsis GNARLED encodes a NAP125 homolog that positively regulates ARP2/3. Curr. Biol. **14,** 1405–1409.

Feenstra, W.J. (1978). Contiguity of linkage groups I and IV as revealed by linkage relationship of two newly isolated markers *dis-1* and *dis-2*. Arabidopsis Inf. Serv. **15,** 35–38.

Frank, M., Egile, C., Dyachok, J., Djakovic, S., Nolasco, M., Li, R., and Smith, L.G. (2005). Activation of Arp2/3 complex-dependent actin polymerization by plant proteins distantly related to Scar/WAVE. Proc. Natl. Acad. Sci. USA **101,** 16379–16384.

Frank, M.J., Cartwright, H.N., and Smith, L.G. (2003). Three Brick genes have distinct functions in a common pathway promoting polarized cell division and cell morphogenesis in the maize leaf epidermis. Development **130,** 753–762.

Frank, M.J., and Smith, L.G. (2002). A small, novel protein highly conserved in plants and animals promotes the polarized growth and division of maize leaf epidermal cells. Curr. Biol. **12,** 849–853.

Gautreau, A., Ho, H.Y., Li, J., Steen, H., Gygi, S.P., and Kirschner, M.W. (2004). Purification and architecture of the ubiquitous Wave complex. Proc. Natl. Acad. Sci. USA **101,** 4379–4383.

Higgs, H.N., and Pollard, T.D. (1999). Regulation of actin polymerization by Arp2/3 complex and WASp/Scar proteins. J. Biol. Chem. **274,** 32531–32534.

Hülskamp, M., Miséra, S., and Jürgens, G. (1994). Genetic dissection of trichome cell development in Arabidopsis. Cell **76,** 555–566.

Innocenti, M., Zucconi, A., Disanza, A., Frittoli, E., Areces, L.B., Steffen, A., Stradal, T.E., Di Fiore, P.P., Carlier, M.F., and Scita, G. (2004). Abi1 is essential for the formation and activation of a WAVE2 signalling complex. Nat. Cell Biol. **6,** 319–327.

Jackson, D. (1991). *In situ* hybridization in plants. In Molecular Plant Pathology: A Practical Approach, D.J. Bowles, S.J. Gurr, and M. McPherson, eds (Oxford: Oxford University Press), pp. 163–174.

Kunda, P., Craig, G., Dominguez, V., and Baum, B. (2003). Abi, Sra1, and Kette control the stability and localization of SCAR/WAVE to regulate the formation of actin-based protrusions. Curr. Biol. **13,** 1867–1875.

Larkin, J.C., Oppenheimer, D.G., and Marks, M.D. (1994). The *GL1* gene and the trichome developmental pathway in *Arabidopsis thaliana*. In Plant Promoters and Transcription Factors, L. Nover, ed (Berlin: Springer-Verlag), pp. 259–275.

Le, J., El-Assal Sel, D., Basu, D., Saad, M.E., and Szymanski, D.B. (2003). Requirements for Arabidopsis ATARP2 and ATARP3 during epidermal development. Curr. Biol. **13,** 1341–1347.

Li, S., Blanchoin, L., Yang, Z., and Lord, E.M. (2003). The putative Arabidopsis arp2/3 complex controls leaf cell morphogenesis. Plant Physiol. **132,** 2034–2044.

Machesky, L.M., Atkinson, S.J., Ampe, C., Vandekerckhove, J., and Pollard, T.D. (1994). Purification of a cortical complex containing two unconventional actins from Acanthamoeba by affinity chromatography on profilin-agarose. J. Cell Biol. **127,** 107–115.

Machesky, L.M., and Gould, K.L. (1999). The Arp2/3 complex: A multifunctional actin organizer. Curr. Opin. Cell Biol. **11,** 117–121.

Mathur, J., Mathur, N., Kernebeck, B., and Hulskamp, M. (2003a). Mutations in actin-related proteins 2 and 3 affect cell shape development in Arabidopsis. Plant Cell **15,** 1632–1645.

Mathur, J., Mathur, N., Kirik, V., Kernebeck, B., Srinivas, B.P., and Hulskamp, M. (2003b). Arabidopsis CROOKED encodes for the smallest subunit of the ARP2/3 complex and controls cell shape by region specific fine F-actin formation. Development **130,** 3137–3146.

Mathur, J., Spielhofer, P., Kost, B., and Chua, N.-H. (1999). The actin cytoskeleton is required to elaborate and maintain spatial patterning during trichome cell morphogenesis in *Arabidopsis thaliana*. Development **126,** 5559–5568.

Oda, A., et al. (2004). WAVE/Scars in Platelets. Blood **105,** 3141–3148.

Oppenheimer, D.G., Pollock, M.A., Vacik, J., Szymanski, D.B., Ericson, B., Feldmann, K., and Marks, M.D. (1997). Essential role of a kinesin-like protein in Arabidopsis trichome morphogenesis. Proc. Natl. Acad. Sci. USA **94,** 6261–6266.

Pollard, T.D., and Borisy, G.G. (2003). Cellular motility driven by assembly and disassembly of actin filaments. Cell **112,** 453–465.

Pollock, M.A., and Oppenheimer, D.G. (1999). Inexpensive alternative to M&S medium for selection of Arabidopsis plants in culture. Biotechniques **26,** 254–257.

Rogers, S.L., Wiedemann, U., Stuurman, N., and Vale, R.D. (2003). Molecular requirements for actin-based lamella formation in Drosophila S2 cells. J. Cell Biol. **162,** 1079–1088.

Saedler, R., Mathur, N., Srinivas, B.P., Kernebeck, B., Hulskamp, M., and Mathur, J. (2004). Actin control over microtubules suggested by DISTORTED2 encoding the Arabidopsis ARPC2 subunit homolog. Plant Cell Physiol. **45,** 813–822.

Schwab, B., Folkers, U., Ilgenfritz, H., and Hulskamp, M. (2000). Trichome morphogenesis in Arabidopsis. Philos. Trans. R. Soc. Lond. B Biol. Sci. **355,** 879–883.

Schwab, B., Mathur, J., Saedler, R., Schwarz, H., Frey, B., Scheidegger, C., and Hulskamp, M. (2003). Regulation of cell expansion by the DISTORTED genes in *Arabidopsis thaliana*: Actin controls the spatial organization of microtubules. Mol. Genet. Genomics **269,** 350–360.

Smith, L.G. (2003). Cytoskeletal control of plant cell shape: Getting the fine points. Curr. Opin. Plant Biol. **6,** 63–73.

Steffen, A., Rottner, K., Ehinger, J., Innocenti, M., Scita, G., Wehland, J., and Stradal, T.E. (2004). Sra-1 and Nap1 link Rac to actin assembly driving lamellipodia formation. EMBO J. **23,** 749–759.

Sugimoto, K., Williamson, R.E., and Wasteneys, G.O. (2000). New techniques enable comparative analysis of microtubule orientation, wall texture, and growth rate in intact roots of Arabidopsis. Plant Physiol. **124,** 1493–1506.

Szymanski, D.B., Jilk, R.A., Pollock, S.M., and Marks, M.D. (1998). Control of *GL2* expression in *Arabidopsis* leaves and trichomes. Development **125,** 1161–1171.

Szymanski, D.B., Lloyd, A.M., and Marks, M.D. (2000). Progress in the molecular genetic analysis of trichome initiation and morphogenesis in *Arabidopsis*. Trends Plant Sci. **5,** 214–219.

Szymanski, D.B., Marks, M.D., and Wick, S.M. (1999). Organized F-Actin is essential for normal trichome morphogenesis in Arabidopsis. Plant Cell **11,** 2331–2348.

von Arnim, A.G., Deng, X.-W., and Stacey, M.G. (1998). Cloning vectors for the expression of green fluorescent protein fusion proteins in transgenic plants. Gene **221,** 35–43.

Wasteneys, G.O. (2000). The cytoskeleton and growth polarity. Curr. Opin. Plant Biol. **3,** 503–511.

Weaver, A.M., Young, M.E., Lee, W.L., and Cooper, J.A. (2003). Integration of signals to the Arp2/3 complex. Curr. Opin. Cell Biol. **15,** 23–30.

Zhang, X., and Oppenheimer, D.G. (2004). A simple and efficient method for isolating trichomes for downstream analyses. Plant Cell Physiol. **45,** 221–224.